Study of High-energy Ion Tail Formation with Second Harmonic ICRF Heating and NBI in LHD

K. Saito[1)], S. Murakami[2)], M. Osakabe[1)], M, Nishiura[1)], T. Seki[1)], T. Ozaki[1)], P. Goncharov[1)], M. Sasao[3)], H. Nishimura[3)], M. Isobe[1)], S. Kobayashi[4)], T. Tokuzawa[1)], N. Tamura[1)], R. Kumazawa[1)], T. Mutoh[1)], O. Kaneko[1)], Y. Takeiri[1)], Y. Oka[1)], K. Tsumori[1)], K. Ikeda[1)], K. Nagaoka[1)], H. Yamada[1)], A. Komori[1)], S. Sudo[1)], O. Motojima[1)], and LHD Experimental Group

1) National Institute for Fusion Science, Toki 509-5292, Japan.
2) Department of Nuclear Engineering, Kyoto University, Kyoto 606-8501, Japan.
3) Graduate School of Engineering, Tohoku University, Sendai 980-8579, Japan.
4) Institute of Advanced Energy, Kyoto University, Uji, 611-0011, Japan.

e-mail contact of main author: saito@nifs.ac.jp

Abstract. Ion cyclotron range of frequencies (ICRF) heating is a good tool for the α-particle simulation of a future fusion reactor. In the Large Helical Device (LHD), enhancement of the high-energy ion tail formed by second harmonic ICRF heating by reducing the magnetic field strength was observed in the presence of energetic particles having a large Larmor radius supplied by a perpendicular NBI. Moreover, it was clarified by a pellet charge exchange (PCX) measurement that high-energy deeply trapped particles exist near the ion cyclotron resonance layer. The power modulation experiments clarified the large particle loss due to the large Larmor radius normalized by the plasma minor radius ρ_i*. The spectrum of the high-energy ion tail was consistent with the calculation by the GNET code in the ρ_i* region lower than 0.065. This experimental result supports the GNET simulation that α-particles will be well confined in the heliotron reactor.

1. Introduction

The study of α-particle confinement in reactors is of major importance. Ion cyclotron range of frequency (ICRF) heating is a good tool for α-particle simulation. Higher harmonic ICRF heating is efficient for producing a high-energy ion tail due to the finite Larmor radius effect. Particle acceleration by the n^{th} harmonic wave, which is perpendicular to the magnetic field, is dependent on the n-1 order Bessel function with the argument of $k_\perp\rho_i$. Therefore, particles with a large Larmor radius are more efficiently accelerated with higher harmonic ICRF heating than with fundamental heating. The tail temperature is expected to increase with increasing energy; therefore, it would be easier to detect higher-energy particles than those produced by fundamental ICRF heating. In the Large Helical Device (LHD) [1, 2], minority ion ICRF heating by the fundamental wave is an efficient plasma heating method, and a good confinement of high-energy particles has been proven [3-5]. Second harmonic ICRF heating has been conducted with target plasma heated by a tangential neutral beam injection (NBI) by lowering the magnetic field strength. In this combination of heating methods, the population of particles with a large Larmor radius was small. The high-energy ion tail is expected to be enhanced by accelerating ‘seed’ particles with a large Larmor radius. The ‘seed’ particles can be the high-energy particles accelerated by the minority ion heating or the particles with the large Larmor radius supplied by NBI [6]. The experiment was conducted with the latter method.

There are three heating systems in the LHD: NBI heating, electron cyclotron heating (ECH), and ICRF heating. Two pairs of ICRF loop antennas were located in the vertically elongated plasma section in the LHD, with the antenna straps perpendicular to the toroidal direction in order to launch the fast wave. RF power was fed into the ICRF antennas from the upper and lower ports of the LHD.In the LHD, helium and hydrogen were supplied by gas puffing. In a previous study, a high heating efficiency (absorbed power/injected power) of 80% was obtained by the minority ion heating (hydrogen as minority ions and helium as majority ions) at a frequency of 38.47 MHz and a magnetic field strength on axis B_{ax} of 2.75 T [3]. At that time the ion cyclotron resonance layers in front of the ICRF antenna were located near the saddle point of the mod B contour, where the gradient of the magnetic field strength was small. Plasma with a stored energy of 240 kJ was achieved with an ICRF power of 2.3 MW [7]. Therefore, the second harmonic heating experiments were mainly conducted with this position of the ion cyclotron resonance layer.

In addition to the tangential NBIs, a perpendicular NBI was installed in 2005 in the horizontally elongated plasma section. The energy of the injected hydrogen is 40 keV, and the maximum power with two positive ion sources is 3 MW.

High-energy particle detectors, such as silicon-diode-based fast neutral analyzers (SiFNA) [8], natural diamond detectors (NDD) [9], and a compact neutral particle analyzer (CNPA) were installed on the LHD. In addition to the passive measurements, the CNPA in combination of a polystyrene pellet injection was used for the pellet charge exchange (PCX) measurement [10, 11] to determine the distribution of high-energy particles. In Fig. 1, the positions of the ICRF antennas, NBI injectors, and high-energy particle detectors are shown.

In Section 2, we discuss the enhancement of high-energy ion tail formation by the perpendicular NBI. The distribution of deeply trapped particles measured by the PCX is shown in Section 3. In section 4 we describe the behavior of high-energy ions during ICRF power modulation. The result of the calculation by the GNET code is discussed in Section 5. Section 6 is a summary.

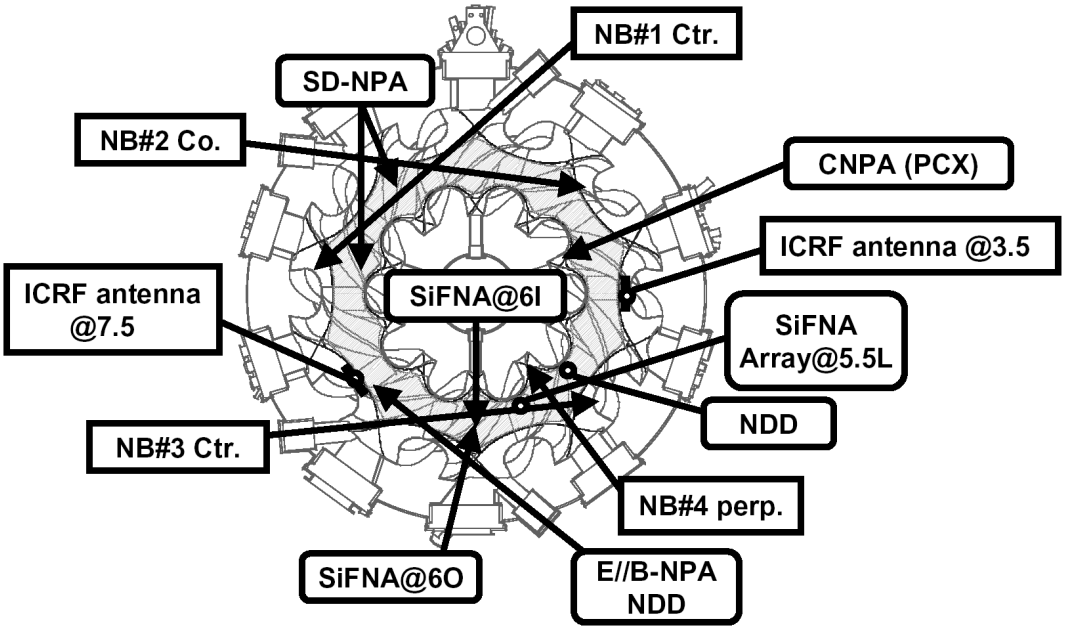

Fig. 1 Positions of ICRF antennas, NBI injectors, and high-energy particle detectors.

2. Enhancement of the High-energy Ion Tail

The second harmonic ICRF power was launched into the plasma sustained by the tangentially injected NBI, as shown in Fig. 2. The resonant particle was the hydrogen ion. The applied ICRF frequency was 38.47 MHz, and the magnetic field strength on the axis was 1.375 T. A pair of second harmonic ion cyclotron resonance layers were located at the off-axis, as shown in Fig. 3.

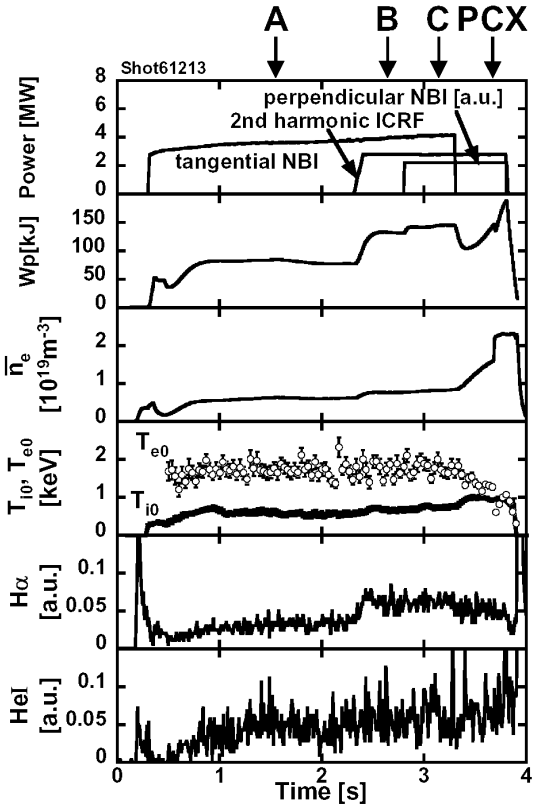

Fig. 2 Experiment of second harmonic ICRF heating with NBI heating.

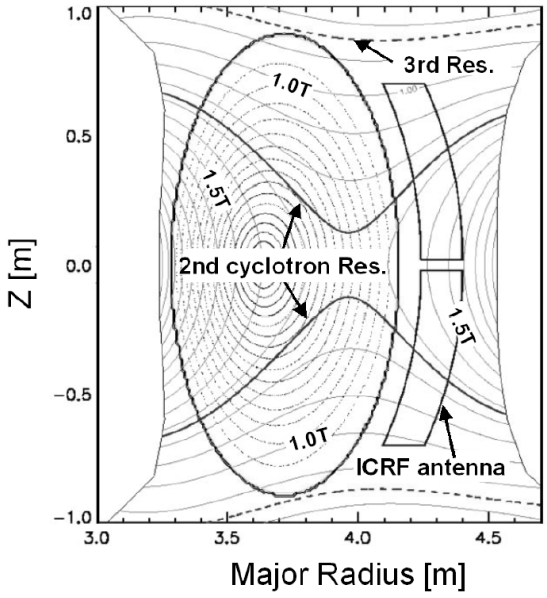

Fig. 3 The magnetic field strength and ion cyclotron resonance layers in front of the ICRF antenna.

The innermost normalized minor radius of the resonance layers was 0.5. The seed particles of hydrogen were injected at 2.8 seconds by the perpendicular NBI with an energy of 40 keV. The ICRF heating power and the perpendicular NBI power were 2.7 MW and 2.2 MW, respectively. At the time of the injection of the perpendicular NBI, the plasma stored energy was approximately 150 kJ, and the line-averaged electron density was 0.8×10^{19} m^{-3}. Electron and ion temperatures were 1.8 keV and 0.7 keV, respectively. Figure 4(a) shows the relationship between the particle energy and the particle counts measured by the SiFNA at 6I port in 0.3 seconds at the time of A, B, and C indicated by arrows in Fig. 2. The SiFNA detects high-energy ions with the perpendicular pitch angle that escape from the plasma by the charge exchange reaction. The number of the high-energy ions with the perpendicular pitch angle generated only with the tangential beam was small. However, by the second harmonic ICRF heating, the high-energy ion tail was enlarged. It was found that the detected counts increased by a factor of three in the presence of the perpendicular NBI. The emission from the neutral particles in the same helical section with the SiFNA was not changed by the injection of the perpendicular NBI, as shown in the bottom two graphs in Fig. 2. Therefore, the charge exchange rate was constant, and the increase in the detected counts is caused by an increase in the population of high-energy ion tail. Figure 4(b) shows the

relationship between the Larmor radius normalized by the plasma minor radius ρ_i*, a key parameter for the orbital loss of high-energy particles, and the detected particle counts. The operational ρ_i* region was increased by the injection of the perpendicular NBI. The case of minority ion heating of similar parameters with strong magnetic strength (B_{ax}=2.75 T) is also shown. The value of ρ_i* for the α-particles produced by the D-T reaction at the heliotron reactor FFHR2m1 [12] was estimated to be ρ_α*=0.025. Therefore, the high-energy particle confinement can be investigated within a sufficient margin.

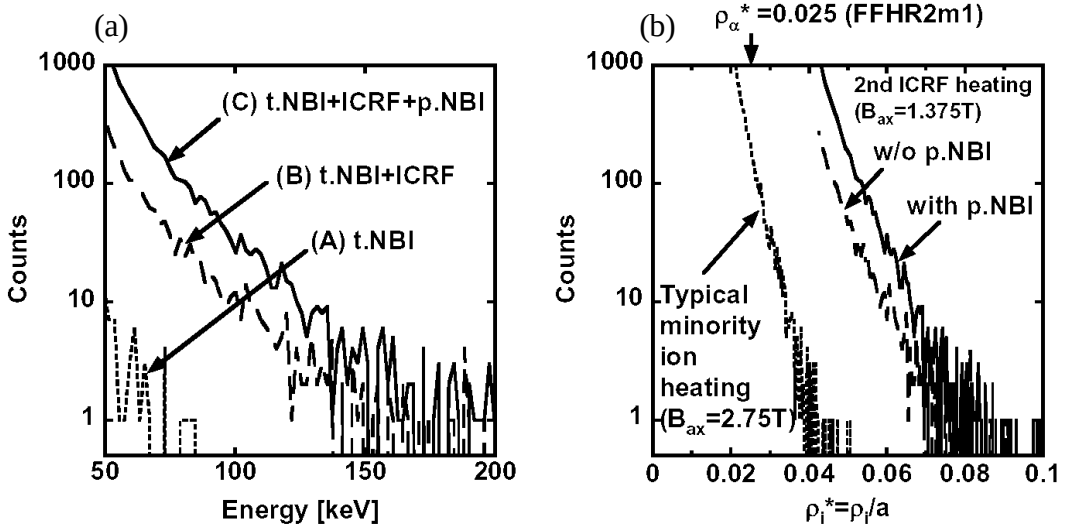

Fig. 4 Enhancement of ion tail. (a) Energy spectrum of high-energy particles. (b) Particle counts v.s. normalized Larmor radius ρ_i.*

When the ion cyclotron resonance layer was located on the magnetic axis, the high-energy ion tail measured by the NDD was smaller than that of the off-axis heating, as shown in Fig. 5(a) and (b). This result is the same with the minority ion heating and is explained as follows. In the off-axis heating case (B_{ax}=1.375 T), the particles that have turning points on the cyclotron resonance layer are deeply trapped in the helical ripple at a normalized minor radius of 0.5. However, in the on-axis heating case (B_{ax}=1.25 T), these particles are trapped-detrapped particles and are easily diffused since the magnetic field at the top of the helical ripple is reduced even though it is the same resonant magnetic field.

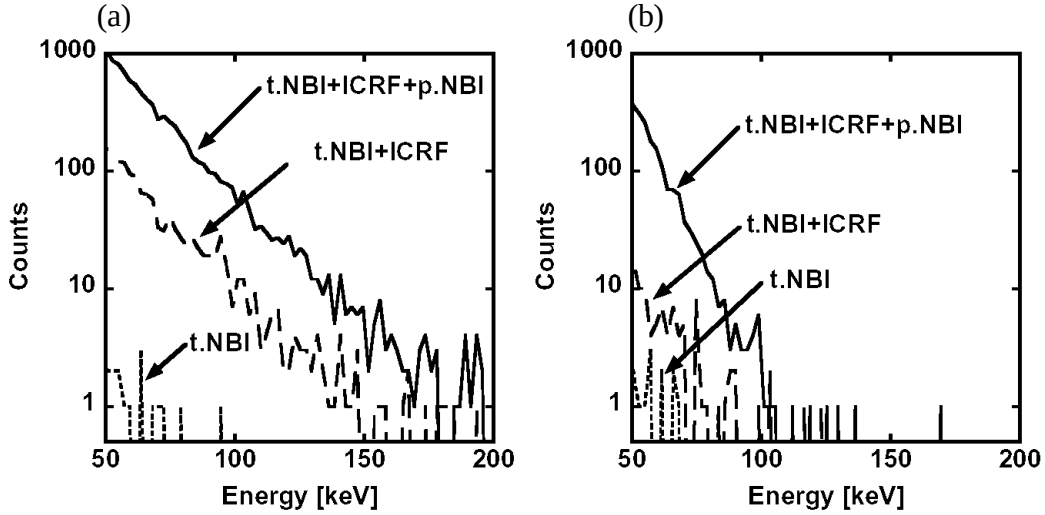

Fig. 5 Difference of tail formations between (a) off-axis heating and (b) on-axis heating.

3. High-energy Ion Distribution

The high-energy ion distribution was measured by the PCX method. The cloud of the polystyrene pellet injected into the plasma increases the local charge exchange rate. It provides a local measurement of the high-energy ions with a perpendicular pitch angle by using CNPA, which has a high time resolution of 100 μs and 40 energy channels from 0.8 keV to 168 keV.

It was found that the low energy particles supplied by the perpendicular NBI existed in the wide plasma region, as shown in Fig. 6(a). The pellet was injected into the plasma at a time of 3.688 s, as indicated by an arrow in Fig. 3, and the distribution of high-energy ions by the second harmonic ICRF heating in the presence of the perpendicular NBI was measured with the CNPA, as shown in Fig. 6(b). The fluxes of high-energy particles have a maximum at a normalized minor radius ρ of approximately 0.5. This position agrees with the ion cyclotron resonance layer on the line of sight of CNPA.

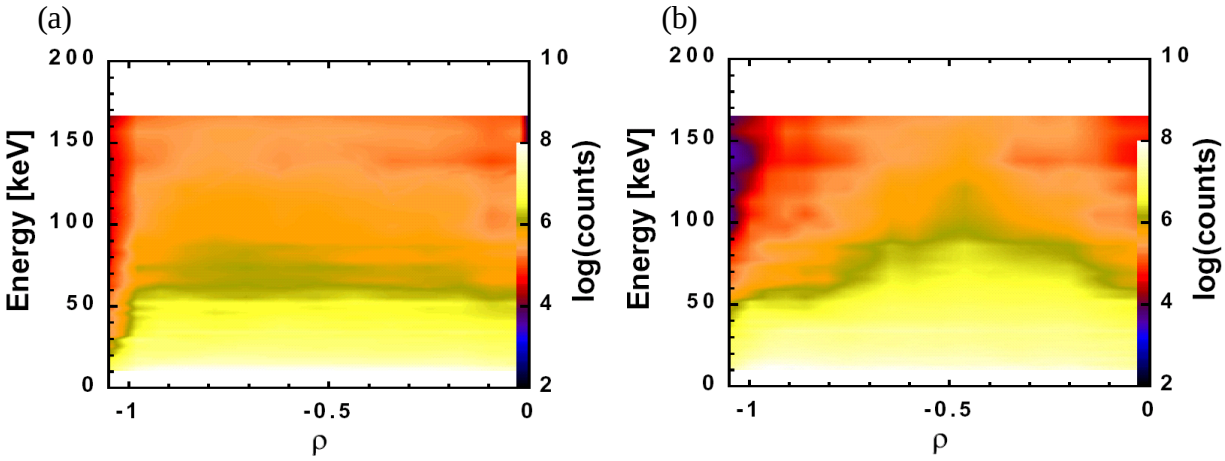

Fig. 6 Distribution of high-energy ions measured by PCX. (a) Perpendicular NBI only. (b) With second harmonic ICRF heating. The ion cyclotron resonance layer locates at ρ=0.5.

4. Behavior of High-energy Ions in Power Modulation

To study the transient behavior of high-energy ions, a power modulation experiment was conducted. ICRF heating was superposed on the tangential NBI with the power modulation of a sin wave, as shown in Fig. 7. The modulation frequency was 4 Hz. At the time of 1.8 seconds, the perpendicular NBI was injected. The high-energy flux measured by the CNPA increased, and fluctuation was clearly observed, as shown in the bottom graph of Fig. 7. A phase difference between the modulated ICRF heating power and the fluctuated particle flux from 2.0 to 2.5 seconds is plotted by circles in Fig. 8. It was found that the phase delay relative to the ICRF heating power was approximately 20°. A distribution function f was solved by a bounce-averaged Fokker-Planck equation [13] to simulate this phase delay. For the simplicity of the calculation, a helical symmetrical magnetic configuration was employed. A bounce-averaged Fokker-Planck equation is obtained by integrating the local RF kick term Q and the collision term C along the magnetic line of force with an approximation based on assuming no deviation of the particle orbit from the magnetic flux surface. Since the orbital loss is not included, the artificial loss was added to the bounce-averaged RF kick term $\overline{Q}$ and collision term $\overline{C}$ as well as the source and sink

term S as follows:

$$\partial f / \partial t = \overline{Q}(f) + \overline{C}(f) + S - f / \tau_{loss}.$$

The loss time τ_{loss} was set to be inversely proportional to the particle energy, assuming that the loss is proportional to the square of ρ_i*. The calculation was conducted using the plasma parameters at the innermost cyclotron resonance layer according to the PCX measurement described in Section 3. The tangential NBI was not included in this calculation. The RF field and the source of the perpendicular NBI were determined to meet the experimental effective temperature of the ion tail at an energy of around 100 keV and an enhancement factor by the perpendicular NBI, respectively. The efficiency of the power transmission from high-energy ions to bulk plasma η was also obtained by calculating the transferred power and the lost power using the collision term and the loss term, respectively. The phase delay decreased with a decreasing η, as shown by the lines in Fig. 8. The experimental result and the calculation agreed at η=0.2. In minority ion heating at a magnetic field strength of 2.75 T, the tail energy was almost absorbed by the bulk plasma at a power of 0.5 MW and an electron density of 1.0×10^{19} m^{-3} [5]. It is thought that the low efficiency in the second harmonic heating is due to the large ρ_i*, as shown in Fig. 4(b).

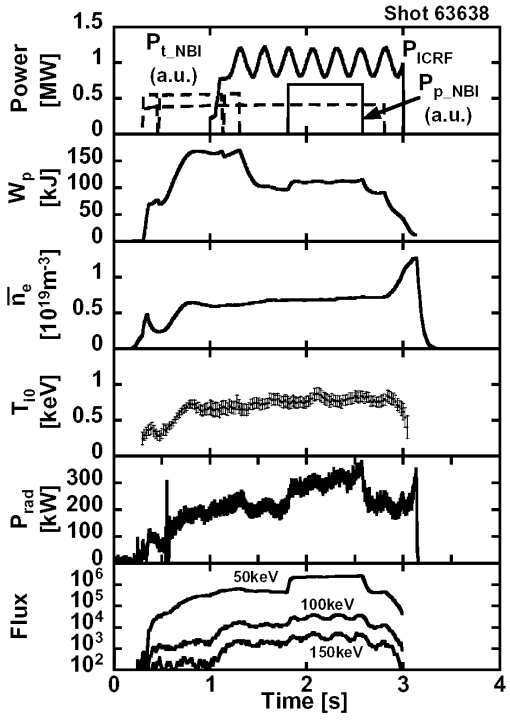

Fig. 7 The power modulation experiment of the second harmonic ICRF heating.

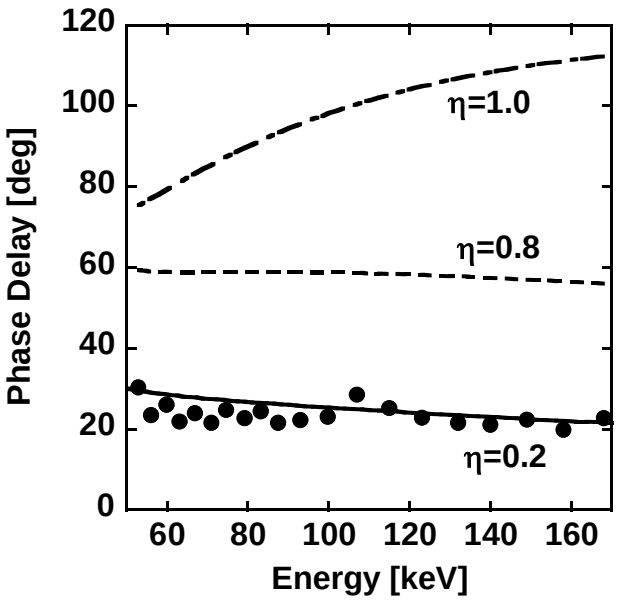

Fig. 8 The phase delay of the high-energy particle flux relative to the ICRF heating power.

The gradients of the energy spectrum obtained by the experiments were the same with and without the perpendicular NBI, as shown in Fig. 4(a), which is also explained by the Fokker-Planck equation. The Fokker-Planck equation of a steady-state condition at an energy higher than the source energy is written as follows:

$$0 = \overline{Q}(f) + \overline{C}(f) - f / \tau_{loss}.$$

The gradients of the log f in the high-energy region are the same regardless of whether the source exists since the terms $\overline{Q}$ and $\overline{C}$ are the linear functions of f. Therefore, the population of the particles with an energy much higher than the source energy could be enhanced.

5. Simulation by GNET Code

Particle counts measured by the NDD were simulated by using the global simulation code, GNET [14-16], which solves a drift kinetic equation in 3D space and 2D velocity space based on the Monte Carlo technique. The particle source term by NBI was evaluated by the NBI heating analysis code, HFREYA [17]. The dashed line in Fig. 9 is the simulated counts in the case of second harmonic ICRF heating with tangential NBI heating. By adding the perpendicular NBI, counts were increased, as shown by the solid line. The enhancement of the ion tail is the same for both the experiment and the GNET code. The gradient of the experimental counts is comparable to that of the simulation in the region below ρ_i*=0.065, although the discrepancy is seen in the larger ρ_i* region. Therefore, the evaluation of orbital loss by GNET is reasonable in the region below ρ_i*=0.065. Since ρ_α* is 0.025 in the helical reactor, the experimental result supports the prediction of the GNET code that α-particles will be well confined in the heliotron reactor [15].

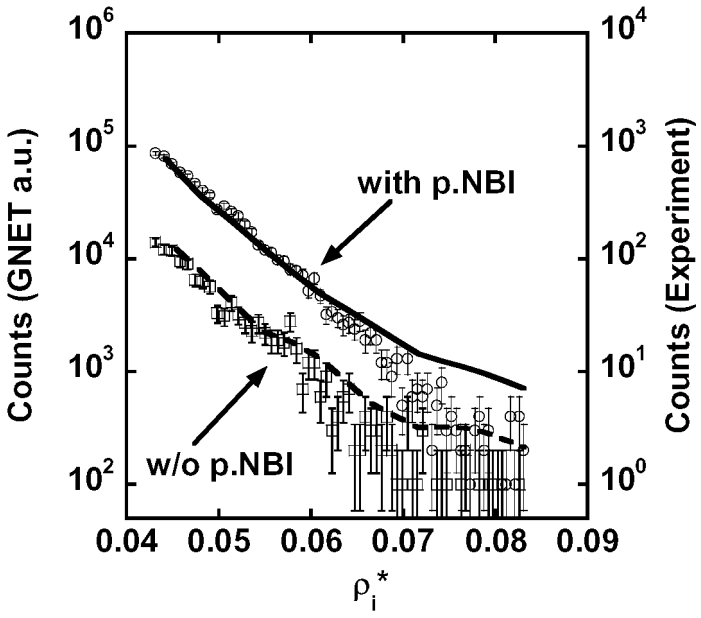

Fig. 9 Simulated counts by GNET code (dashed and solid lines) and the experimental counts in 0.3 seconds (squares and circles).

6. Summary

By the injection of perpendicular NBI with an energy of 40 keV, the high-energy ion tail formed by the second harmonic ICRF heating was enhanced. The off-axis heating had a better confinement performance than the on-axis heating. The high-energy ion distribution was measured by the PCX, which clarified that the high-energy deeply trapped particles accelerated by second harmonic ICRF heating are mainly located at the ion cyclotron resonance layer. The large loss was clarified in the second harmonic ICRF heating by the power modulation experiment. By increasing the magnetic field strength, however, the confinement of high-energy particles will be improved, and a large ion tail is expected. Particle counts measured by the NDD were simulated by using the GNET code. The simulation and experiment agreed in the region below ρ_i*=0.065. This experimental result supports the GNET simulation that α-particles will be well confined in the heliotron reactor.

Acknowledgements

The authors would like to thank the technical staff of the LHD group of the National Institute for Fusion Science for their helpful support during this work. This work was supported by NIFS budget NIFS05ULRR504-508 and NIFS05ULBB501.

References

[1] Motojima, O., et al., Fusion Sci. Technol. **46** (2004) 1.
[2] Komori, A., et al., Fusion Sci. Technol. **50** (2006) 136.
[3] Saito, K., et al., Nucl. Fusion **41** (2001) 1021.
[4] Saito, K., et al., Plasma Phys. Control. Fusion **44** (2002) 103.
[5] Kumazawa, R., et al., Plasma Phys. Control. Fusion **45**(2003)1037.
[6] Mantsinen, M., Mayoral, M.-L., et al., Phys. Rev. Letters **88** (2002) 105002-1.
[7] Seki, T., et al., Proc. of 14th Top. Conf. on RF Power in Plasmas **595** (2001) 67.
[8] Osakabe, M., et al., Rev. Sci. Instrum. **72** (2001) 788.
[9] Isobe, M., et al., Rev. Sci. Instrum. **72** (2001) 611.
[10] Goncharov, P. R., et al., Rev. Sci. Instrum. **74** (2003) 1869.
[11] Goncharov, P. R., et al., Fusion Sci. Technol. **50** (2006) 222.
[12] Sagara, A., et al., Nucl. Fusion **45** (2005) 258.
[13] Stix, T.H., WAVES IN PLASMAS, AIP (1992), p521.
[14] Murakami, S., et al., Nucl. Fusion **40** (2000) 693.
[15] Murakami, S., et al., Fusion Sci. Technol. **46** (2004) 241.
[16] Murakami, S., et al., Nucl. Fusion **46** (2006) S425-S432.
[17] Murakami, S., Nakajima, N., Okamoto, M., Fusion Technology **27** Suppl. S (1995) 256.